Helium Exhaust and Forced Flow Effects with Both-leg Pumping in W-shaped Divertor of JT-60U

A. Sakasai, H. Takenaga, S. Higashijima, H. Kubo, T. Nakano, H. Tamai, S. Sakurai,
N. Akino, T. Fujita, N. Asakura, K. Itami, K. Shimizu, the JT-60 Team

Japan Atomic Energy Research Institute, Naka Fusion Research Establishment
Naka-machi, Naka-gun, Ibaraki-ken, 311-0193 JAPAN

e-mail contact of main author: sakasai@naka.jaeri.go.jp

Abstract. The W-shaped divertor of JT-60U was modified from inner-leg pumping to both-leg pumping. After the modification, the pumping rate was improved from 3% with inner-leg pumping to 5% with both-leg pumping in a divertor-closure configuration, which means both separatrixes close to the divertor slots. Efficient helium exhaust was realized in the divertor-closure configuration with both-leg pumping. A global particle confinement time of τ^*_{He} = 0.4 s and τ^*_{He}/τ_E = 3 was achieved in attached ELMy H-mode plasmas. The helium exhaust efficiency with both-leg pumping was extended by 45% as compared with inner-leg pumping. By using central helium fueling with He-beam injection, the helium removal from the core plasma inside the internal transport barrier (ITB) in reversed shear plasmas in the divertor-closure configuration was investigated for the first time. The helium density profiles inside the ITB were peaked as compared with those in ELMy H-mode plasmas. In the case of low recycling divertor, it was difficult to achieve good helium exhaust capability in reversed shear plasmas with ITB. However, the helium exhaust efficiency was improved with high recycling divertor. Carbon impurity reduction was observed by the forced flow with gas puff and effective divertor pumping.

1. Introduction

Control of helium (He) ash is one of the key issues in ITER-FEAT [1] and future tokamak reactors, such as SSTR (Steady State Tokamak Reactor) [2]. ITER-FEAT is designed to operate in ELMy H-modes or some other enhanced confinement regime for helium ash exhaust. A detailed experimental database related to He level regulation and He ash removal should be developed to contribute to the determination of the device size and to the evaluation of the margin to ignition achievement. ELMy H-mode is attractive because of its capability of steady-state operation and particle exhaust by MHD relaxation at the plasma peripheral region.

In previous helium exhaust studies on JT-60U with He beam fueling, good He exhaust capability (τ^*_{He}/τ_E = 4) was successfully demonstrated in ELMy H-mode plasmas with the W-shaped divertor in steady state [3, 4]. The enrichment factor of He was estimated to be about 1.0, which is 5 times larger than the ITER requirement of 0.2. The enrichment factor of He was defined by $\eta_{He} = [P_{He}/2P_{D2}]_{div}/[n_{He}/n_e]_{main}$, where $[P_{He}/2P_{D2}]_{div}$ is the ratio of the He neutral pressure to the deuterium neutral pressure in the divertor and $[n_{He}/n_e]_{main}$ is the ratio of the He density to the electron density in the main plasma. Helium transport in ELMy H-mode and reversed shear discharges has been investigated [4, 5].

Reversed shear mode with ITB is attractive because of its high performance and a large fraction of bootstrap currents in non-inductive current drive as one of advanced tokamak operation scenarios for future steady-state tokamak reactors, such as ITER-FEAT. However, helium ash exhaust from the revered shear plasma is a matter of concern. A previous study of

He exhaust in reversed shear plasmas using He gas puff indicated that helium removal inside the ITB was 2 - 3 times as difficult as outside the ITB [4]. It is very important to make clear He exhaust characteristics of reversed shear plasma because of an enhancement of He particle confinement.

The W-shaped divertor of JT-60U was modified from inner-leg pumping to both-leg pumping in Nov. - Dec., 1998. After the modification, the pumping rate and the helium exhaust efficiency was improved in a divertor-closure configuration. Helium exhaust experiment was performed to investigate the efficiency of helium exhaust with both-leg pumping in ELMy H-mode discharges. The influence of the pumping gap in a closed divertor on deuterium and helium exhaust was investigated in Alcator C-Mod [6] and ASDEX-U [7]. In this paper, the efficient helium exhaust in ELMy H-mode plasmas with the improvement of the pumping rate, and helium removal from the core plasma inside the internal transport barrier (ITB) in reversed shear plasmas are reported. Carbon impurity reduction by the forced flow with puff and effective divertor pumping are also reported.

2. Modification of W-shaped divertor

The W-shaped divertor of JT-60U was modified from inner-leg pumping to both-leg pumping. In the W-shaped divertor of JT-60U, the outer exhaust slot, which has an aperture of 2 cm, was added to the existing inner one (with an aperture of 3 cm) as shown in Fig. 1(a). In the case of inner-leg pumping, carbon fiber composite (CFC) tiles were used for divertor plates, top tiles of the dome and baffling tiles at the divertor throat, and graphite tiles were used for the other parts so far. Therefore, heat load to the dome bottom exceeded the limited surface temperature 600°C of the graphite tiles in the configuration of the inner/outer separatrix close to the inner/outer slots. The divertor configuration had to be kept with the gap-in and gap-out > 3 cm (i.e. distances between the inner/outer separatrix and the inner/outer slots).

With the modification of the divertor pumping, all tiles of the dome were switched from graphite to CFC to prevent the problem of heat load to the dome bottom tiles. After this modification, a divertor-closure configuration, which means that the gap-in and gap-out are close to 0.5–1.0 cm and the divertor throat become narrow with lower X-point configuration, could be used. The divertor experiments with both-leg pumping were started in February, 1999. The effective pumping speed for both-leg pumping was estimated to be 15.9 m^3/s at about 0.1 Pa by using a gas filling method, which is 25% higher than the one for inner-leg pumping. Helium exhaust is accomplished by condensing an argon (Ar) frost

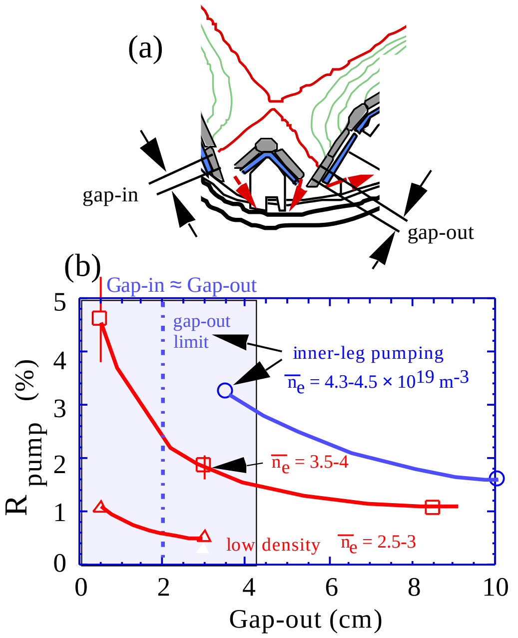

Fig. 1. (a) W-shaped divertor with both-leg pimping in JT-60U and (b) the pumping rate as a function of the gap-out (gap-in ≈ gap-out for both-leg pumping).

layer on the liquid helium cooled surface of three NBI cryopumps for divertor pumping between successive plasma discharges by injecting a known amount of Ar gas into the port chambers.

3. Improvement of Pumping Rate

Previous studies in W-shaped divertor with inner-leg pumping indicated that the private dome and inclined target type divertor was successful in preventing the upstream transport of hydrocarbons generated by chemical sputtering, thereby reducing the resultant carbon influx to the main plasma [8]. The inner-leg pumping was effective in attached divertor because of inboard-enhanced deuterium flux. On the contrary, it was not effective in detached divertor plasma because of a remarkable increase in neutral pressure near the outer strike-point with no pump. Actually, the X-point MARFE onset density was slightly reduced in the W-shaped divertor with inner-leg pumping as compared to the open divertor without pump. With the modification of the both-leg pumping, the onset density of the detachment as well as X-point MARFE gradually increases up to 15% with increasing pumping rate. The pumping rate is defined by the ratio of the deuterium particle flux exhausted with pumping to the deuterium particle flux in the divertor, $R_{pump} = \Phi_{pump} / \Phi_{div}$.

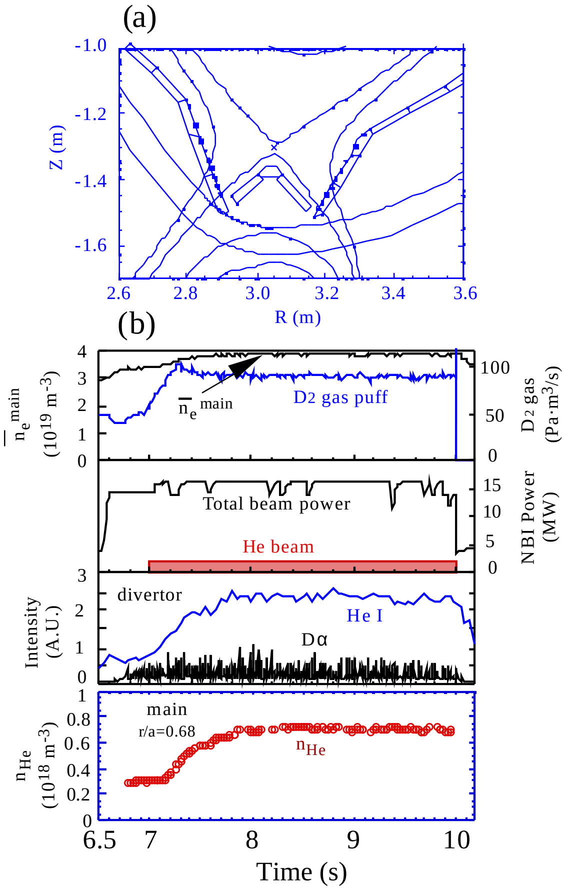

Fig. 2. (a) A divertor-closure configuration with both-leg pumping. (b) Time evolution of the electron density, the fueled D2 gas puff rate, total injected NB power, He I and Dα intensities in the divertor, helium density at r/a = 0.68 in an ELMy H-mode plasma.

Fig 1(b) shows the pumping rate as a function of the gap with both-leg pumping and inner-leg pumping in ELMy H-mode plasmas at I_P=1.5 MA, B_t=3.5 T, P_{NB}=12 MW. After the modification to both-leg pumping, the pumping rate strongly depends on the gap-in and gap-out in L- and H-mode plasmas. Neutral particles accumulated in the inner private region are exhausted through the space under the dome. In the case of large gap-out, the back-flow to the outer divertor occurred through the outer slot and the pumping rate deteriorated. Actually, the pumping rate at the gap-in and gap-out of 3.0 - 3.5 cm with both-leg pumping was estimated to be about 70% of the one at the gap-in of 3.5 cm with inner-leg pumping. In order to improve the pumping rate, the divertor-closure to prevent the back-flow to the outer divertor is key point. The pumping rate was improved up to 5% with both-leg pumping in a divertor-closure configuration at the gap-in and gap-out of 0.5 cm from 3% with inner-leg pumping at $\overline{n}_e$ = $3.5 - 4.0 \times 10^{19}$ m^{-3}. However, the pumping rate reduced to 1% in the lower density region at $\overline{n}_e = 2.5 - 3.0 \times 10^{19}$ m^{-3}. The pumping rate depends on the edge density, which means the particle recycling flux in the divertor. The edge density regime is $n_{e,edge} = 1.5 - 2 \times 10^{19}$ m^{-3} for $\overline{n}_e = 2.5 - 3.5 \times 10^{19}$ m^{-3}.

4. Efficient Helium Exhaust in ELMy H-mode Plasmas

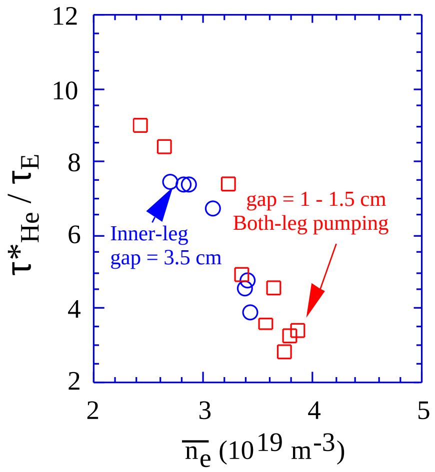

Fig. 3. The ratio of τ^*_{He}/τ_E *as a function of the line-averaged electron density in the main plasma.*

Efficient helium exhaust was realized with He beam injection of $P_{He\text{-}NB}$ = 1.4 MW, which corresponds to He fueling rate of 1.5 × 10^{20} /s (equivalent to 85 MW α heating) for 3 s into ELMy H-mode discharges (I_P = 1.4 MA, B_t = 3.5 T, P_{NB} = 16 MW, q95 = 4.0, V_P = 58 m^3) as shown in Fig.2. Divertor-closure configuration at the gap-in and gap-out of 1 cm was kept constant for 3 s. The line-averaged electron density in the main plasma is $\overline{n}_e = 3.8 \times 10^{19}$ m^{-3}, which corresponds to 0.57 of Greenwald density limit, and the central ion and electron temperatures are $T_i(0)$ = 3.2 keV and $T_e(0)$ = 3.0 keV in the ELMy H-mode plasma. Deuterium gas of about 90 Pa·m^3/s is puffed to keep the electron density constant by a density feedback control. The He concentration reached 2% of the electron density in the main plasma and was kept constant for 2 s.

This indicates that the He source rate (equivalent to 0.6 Pa·m^3/s) from the He beam injection is balanced by the exhaust rate with He pumping. The electron density in the main plasma has a broad profile and high edge density of $\overline{n}_e = 2.5 \times 10^{19}$ m^{-3} (r/a = 0.93). The He density has the same profile as the electron density. In this discharge, τ^*_{He} = 0.36 s and τ^*_{He}/τ_E = 2.8 with τ_E = 0.13 s and an H-factor ($\equiv \tau_E/\tau_E^{ITER\text{-}89P}$) = 1.2 were achieved, well within the range generally considered necessary for successful operation of future fusion reactors, such as ITER-FEAT (i.e., τ^*_{He}/τ_E = 5).

The He exhaust capability was compared between both-leg pumping and inner-leg pumping. The dependence of τ^*_{He} on n_e in the divertor-closure configuration (gap = 0.5 – 1.0 cm) with both-leg pumping is almost same as the one with inner-leg pumping (gap = 3.5 cm). However, the He exhaust efficiency was extended from τ^*_{He} = 0.67 s (P_{NB}=13 MW) with inner-leg pumping to τ^*_{He} = 0.36 s (P_{NB}=16 MW) with the divertor-closure configuration in the higher density region. As a result, the He exhaust efficiency in the divertor-closure configuration was extended by 45% as compared to the one with the inner-leg pumping.

Figure 3 shows the ratio of τ^*_{He}/τ_E as a function of the line-averaged electron density $\overline{n}_e$ in the main plasma. The dependence of τ^*_{He}/τ_E on $\overline{n}_e$ in the divertor-closure configuration is also same as the one with inner-leg pumping. However, the He exhaust capability was extended from τ^*_{He}/τ_E = 3.9 with inner-leg pumping to τ^*_{He}/τ_E = 2.8 with the divertor-closure configuration in the higher density region.

In the He exhaust experiment, gas puff and pump in the divertor-closure configuration was characterized. The particle recycling in the divertor was enhanced with strong gas puff as shown in Fig. 4 (b). Helium exhaust efficinecy was improved with increasing particle recycling in the divertor as shown in Fig. 4 (a). However, the confinement performane in ELMy H-mode plasmas degraded to H = 1.2- 1.3 with strong gas puff. In order to keep higher electron density than $\overline{n}_e = 3.2 \times 10^{19}$ m^{-3} in the divertor-closure configuration, the required gas puff steeply increases up to 120 Pa·m^3/s, which is the maximum gas puff rate. In the low recycling, good He exhaust capability was not achieved. The enhancement of divertor recycling with no confinement degradation is a key point in the He exhaust experiments.

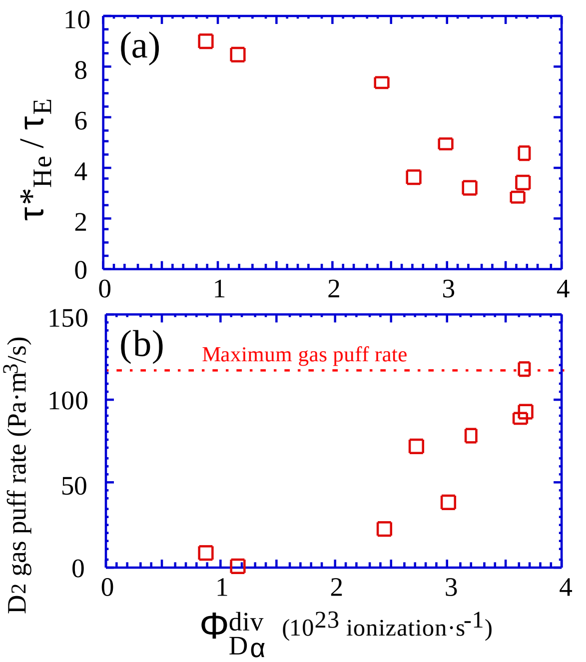

Fig. 4. (a) The D2 gas puff rate required to keep the line-averaged electron density.
(b) The deuterium flux in the divertor from Dα line as a function of the line-averaged electron density.

5. Helium Removal in Reversed Shear Plasmas

In reversed shear modes, the electron density in the central region is peaked and the confinement is remarkably enhanced inside the internal transport barrier (ITB), which is formed near the position of minimum q. Electron density, electron temperature and ion temperature profiles ($n_e(r)$, $T_e(r)$, $T_i(r)$) inside the ITB are peaked in JT-60U [9]. Recently, the stationary reversed shear discharges with H-mode edge was successfully obtained.

Helium removal from core plamsa inside the ITB in reversed shear discharges was investigated with both-leg pumping. Figure 5 shows the time evolution of helium exhaust experiment in reversed shear discharge (I_P = 1.0 MA, B_t = 3.5 T, δ=0.33 and P_{NB} = 7 - 10 MW) by injecting neutral beam of 60 keV helium atoms into the core plasma inside ITB as central fueling of helium for the first time. In this discharge,

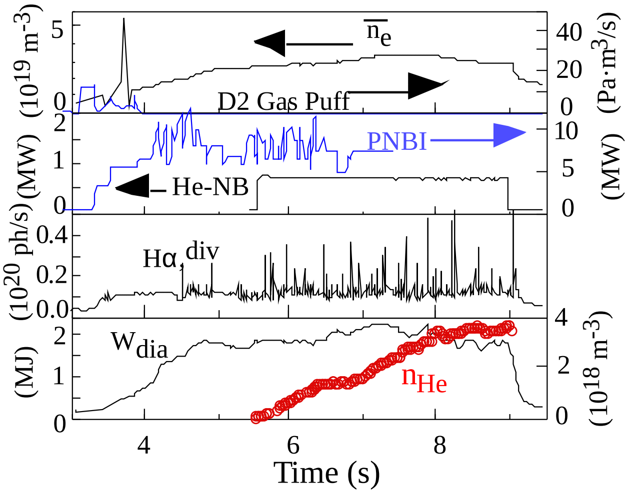

Fig. 5. Typical time evolution of the electron density, the fueled D2 gas puff rate, He-NB and total injected NB power, Da intensities in the divertor, the stored energy and the helium density at r/a = 0.4 in an reversed shear plasma.

the residence time of He density at $r/a < 0.4$ inside the ITB is $\tau = 5.2$ s, while the residence time at $r/a > 0.6$ near the ITB is $\tau = 3.1$ s. The reversed shear plasma had good confinement peformance with H = 2.4 and $\beta_N = 1.44$. The He residence time inside the ITB is longer than that outside the ITB. If the residence time of the He density inside the ITB is assumed as the local τ^*_{He}, the ratio of τ^*_{He}/τ_E was estimated to be 15. The increase in helium density inside the ITB was faster than outside the ITB and helium density profile was gradually peaked. Helium exhaust in reversed shear plasmas in high triangularity configuration was unfavorable to He removal because of only outer-leg pumping. Usually, an inboard-enhanced D flux profile was observed in JT-60U.

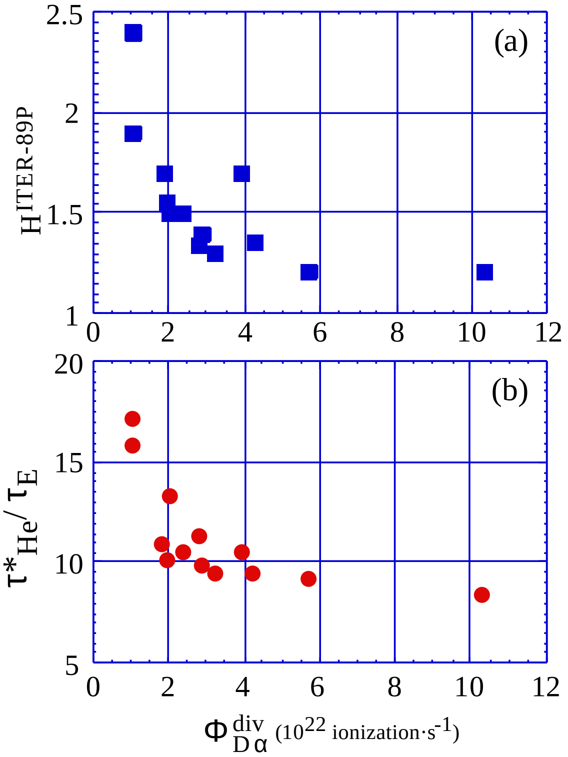

Fig. 6. (a) The H-factor and (b) The ratio of τ^*_{He}/τ_E in RS plasmas with the ITB as a function of the deuterium flux in the divertor.

So, helium exhaust in reversed shear plasmas with high recycling in a divertor closure configuration as well as ELMy H-mode plasmas was addressed. In order to improve the He exhaust efficiency in the core plasma, particle recycling flux was enahanced by D_2 gas puff and a shallow pellet injection. Figure 6 shows (a) the H-factor of reversed shear plasmas and (b) the ratio of τ^*_{He}/τ_E as a function of the deuterium flux in the divertor, where τ^*_{He} is derived on basis of the particle balance from the total He particle number. The confinement performance of reversed shear plasmas with the ITB deteriorated with increasing the deuterium flux. While the ratio of τ^*_{He}/τ_E was reduced with increasing the deuterium flux. The He exhaust efficiency was improved with high recycling divertor. In the highest recycling case (H = 1.2), the ratio of $\tau^*_{He}/\tau_E = 8$ was achieved. It is possible that good He exhaust efficiency with high recycling divertor in a closed divertor coexistes with good confinement. In the W-shaped divertor of JT-60U, the degradation of confinement performance with gas puff is remarkable as compared to DIII-D and JET.

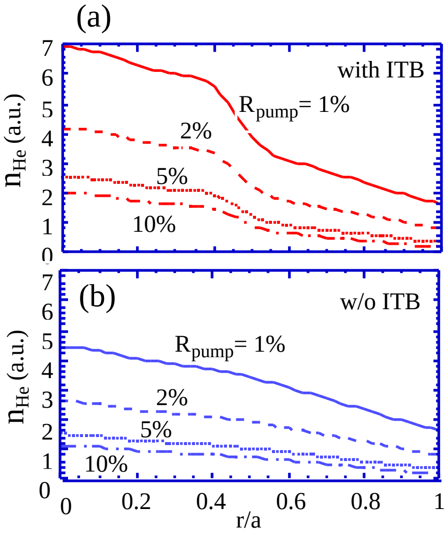

Fig. 7. The calculated He density profiles (a) with ITB and (b) without ITB in the case of the transport coefficient estimated in the gas puff modulation experiment [5] as a function of pumping rate.

A previous study of particle transport

indicated that the particle diffusivity around the ITB was reduced by a factor of 5-6 compared with the inside and outside regions in the reversed shear [5]. A transport analysis was carried out to assess the helium exhaust properties inside the ITB. A one-dimensional, time-dependent, impurity code is employed to calculate helium ion density. The radial diffusion coefficie D(r) an the the convective velocity v (r) are estimated from the results of gas puff modulation experiments. Figure 7 shows the calculated He density profiles with ITB and without ITB. The He density has a peaked profile with ITB. The He density was reduced with increasing pumping rate as well as the one without ITB. Helium removal from the core plasma inside ITB is possible with sufficient pumping rate.

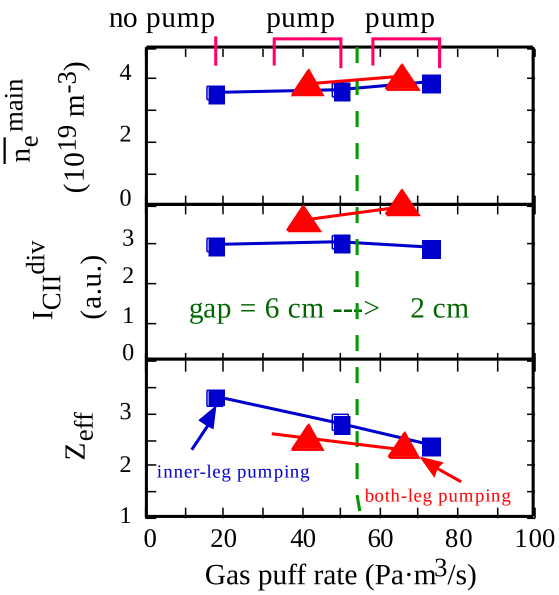

Fig. 8. The electron density, the CII intensity in the divertor, impurity level as a function of gas puff rate for the main plasma.

6. Impurity reduction

Impurity shielding (friction force) with high-density divertor and plasma flow with puff and pump are essential to reduce impurity level in the core plasma. The carbon impurity level in the core plasmas was reduced from Z_{eff} = 3 - 2.6 with inner-leg pumping to Z_{eff} = 2.6 - 2.3 with both-leg pumping at the gas puff rate of 40 - 70 Pa·m^3/s in ELMy H-mode discharges (I_P = 1.2 MA, B_t = 2.5 T, P_{NB} = 18 MW) as shown in Fig. 8. The C II intensity in the divertor with both-leg pumping is larger than that with inner-leg pumping at the same electron density. However, the impurity level with both-leg pumping was lower. Plasma flow with puff and pump (impurity shielding) at the outer divertor may be contributed.

In the case of inner-leg pumping, the X-point MARFE onset density was found to be $\overline{n}_e/n^{Gr}$ = 0.50 [10]. The onset density increased up to $\overline{n}_e/n^{Gr}$ = 0.63 with both-leg pumping in a divertor-closure configuration. The onset density strongly depended on the impurity level. The Z_{eff} < 1.5 was obtained in the case of the higher onset density.

7. Conclusions

The W-shaped divertor of JT-60U was modified from inner-leg pumping to both-leg pumping. After the modification, the pumping rate was improved up to 5% with both-leg pumping in a divertor-closure configuration from 3% with inner-leg pumping at the high density region. In steady state, efficient helium exhaust was realized in a divertor-closure configuration with both-leg pumping in ELMy H-mode plasmas. A global particle confinement time of τ^*_{He} = 0.36 s and τ^*_{He}/τ_E = 2.8 was achieved in attached plasmas. As a result, the He exhaust efficiency in the divertor-closure configuration was extended by 45% as compared to the one with the inner-leg pumping.

Helium exhaust characteristics of reversed shear plasmas has been studied by using He-NB injection in the W-shaped divertor of JT-60U. The helium density profiles inside the ITB were peaked as compared with those in ELMy H-mode plasmas. In the case of low recycling divertor, it was difficult to achieve good helium exhaust capability in reversed shear plasmas with ITB. However, the helium exhaust efficiency was improved with high recycling divertor. Helium removal from the core plasma inside ITB is possible with sufficient pumping rate by the He transport analysis.

Carbon impurity reduction was observed with gas puff and effective divertor pumping. Carbon impurity level was effectively reduced with both-leg pumping.

Acknowledgments

The authors would like to thank the members of the Japan Atomic Energy Research Institute who have contributed to the JT-60 project.

References

[1] Technical Basis for the ITER-FEAT Outline Design Report (Dec. 1999).
[2] M. Kikuchi, Nuclear Fusion 30 (1990) 265.
[3] A. Sakasai et al., Journal of Nuclear Materials 266-269 (1999) 312.
[4] A. Sakasai et al., IAEA Yokohama 1998, IAEA-CN-69/EX6/5.
[5] H. Takenaga et al., Nuclear Fusion 39 (1999) 1917.
[6] J.A. Goetz et al., Journal of Nuclear Materials 266-269 (1999) 354.
[7] H.-S. Bosch et al., Journal of Nuclear Materials 266-269 (1999) 462.
[8] N. Hosogane et al., Journal of Nuclear Materials 266-269 (1999) 296.
[9] Fujita, T. et al., Phys. Rev. Lett. 678 (1997) 237.
[10] S. Higashijima et al., Journal of Nuclear Materials 266-269 (1999) 1078.